Available online at www.sciencedirect.com
SCIENCE DIRECT®
Journal of Sound and Vibration 276 (2004) 293–310
JOURNAL OF SOUND AND VIBRATION
www.elsevier.com/locate/jsvi

Response of block foundations to impact loads

A. Ghafar Chehab, M. Hesham El Naggar*

Department of Civil and Environmental Engineering, Faculty of Engineering, The University of Western Ontario, London, Ont., Canada N6A 5B9

Received 6 March 2003; accepted 27 July 2003

Abstract

Most modern manufacturing facilities have hammers and presses as their production machinery. Foundations supporting hammers and presses experience powerful dynamic effects. These effects may extend to the surrounding and affect laborers, other sensitive machines within the same facility or neighbouring residential areas. The vibration amplitudes and the forces transmitted to the supporting medium can become the governing factor of the foundation of these machines. This paper analyzes the response of one-mass hammer foundations and provides closed-form solutions for their dynamic response to common practical forms of hammer loads: rectangular pulse, half-sine pulse, and triangular pulse. The derived solutions are used to study the effect of the pulse shape and pulse duration on the dynamic response of the one-mass hammer foundation system.

1. Introduction

Foundations supporting hammers, presses and mills experience powerful dynamic effects. These effects are inherent to the forging act of a hammer or the grinding act of a mill and often result in excessive vibrations that may affect the functionality of the machine and cause disturbances in the vicinity of the facility. Therefore, the main objective of the design of a foundation for a shock-producing machine is to reduce the resulting vibrations in the foundation and the supporting medium.

Hammer and mill foundations can be divided into two basic categories: foundations with inertial block (Figs. 1(a) and (b)) and directly sprung machines (Fig. 1(c)). Because of the structural form and rigidity of a hammer foundation, its response analysis is usually performed

*Corresponding author. Tel.: +1519-661-4219; fax: +1519-661-3942.
E-mail address: nagger@uwo.ca (M.H. El Naggar).

0022-460X/$ - see front matter
doi:10.1016/j.jsv.2003.07.028

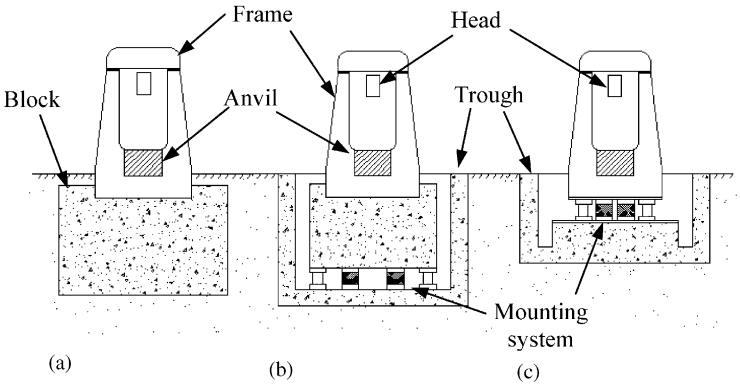

Fig. 1. Typical configurations of the mounting systems in hammer foundations: (a) one-mass foundation, (b, c), two-mass foundation with springs and dampers.

using lumped masses models. Most hammer foundation configurations possess one or two vertical degrees of freedom (assuming centric loading) and are usually modelled as one or two lumped masses with springs and dashpots. A hammer rigidly connected to an inertial block founded on soil or piles (e.g., Fig. 1(a)) may be considered to be a one-mass foundation (i.e., one degree of freedom). A directly sprung hammer founded on rock may also be considered to be a one-mass foundation (e.g., Fig. 1(c) when the supporting medium is rock). Likewise, a clinker mill rigidly connected to its foundation can be considered as a dynamic system in which the mill and foundation behave as a single-mass oscillator with the spring either formed by the ground (or piles) and/or additional spring–damper elements. On the other hand, inertial blocks founded on soil or piles with an elastic pad beneath the anvil, or directly sprung hammers founded on soil or piles may be considered to be two-mass foundations.

The response of hammer foundations under different types of loading has been investigated. Novak [1] and Novak and El Hifnawy [2] investigated the response of one- and two-mass hammer foundation systems. Two methods were used to account for damping in the analysis: a solution based on energy consideration and another based on the complex eigenvalue approach. The effect of the anvil pad flexibility on the foundation response was shown. Novak [1] investigated different configurations of hammer foundations sitting on homogeneous soil or supported by piles. He used the direct method to evaluate the response and the force transmitted into the ground for a one-mass foundation and the modal analysis approach for the two-mass foundations. El Hifnawy and Novak [3] studied the undamped and damped responses of two-mass foundation systems to pulse loading using the complex eigenvalue approach. Chehab and El Naggar [4] investigated the effect of installing a mounting system on the dynamic behaviour of hammer and press foundations and developed design guidelines for efficient mounting systems for hammer foundations using two-mass foundation models.

In this study, closed-form solutions are developed for a one-mass foundation system subjected to the common practical forms of hammer loads: very short-period pulse (i.e., initial velocity approach), rectangular pulse, half-sine pulse, and triangular pulse. These solutions can be used to calculate the exact response time history once the dynamic characteristics of the system are known.

2. Foundation impedance

The foundation impedance can be obtained from the analytical and numerical approaches of the solution of a mixed boundary-value problem in elastodynamics and are generally functions of soil properties, foundation type and size, and exciting frequency.

A number of analytical and numerical approaches, mostly based on the assumption of elastic or viscoelastic soil continuum, are available to calculate the impedance functions for both shallow and deep foundation systems. The impedance function of a foundation system is a complex quantity that has a real part that represents the stiffness and an imaginary (out-of-phase) component that represents the damping. The impedance function of the foundation in the vertical direction can be written as

$$K = k + \mathrm{i}\omega c, \tag{1}$$

where k is the stiffness constant, c is the constant of equivalent viscous damping and ω is the vibration frequency in rad/s.

2.1. Foundation on soil

For embedded foundations in a deep homogeneous stratum (half-space), the stiffness and damping constants can be calculated using the formulae from Refs. [5,6], i.e.,

$$k = Gr_0\left(C_{v1} + \frac{G_s}{G}\frac{l}{r_0}S_{v1}\right), \tag{2a}$$

$$c = r_0^2\sqrt{\rho G}\left(\bar{C}_{v2} + \bar{S}_{v2}\frac{l}{r_0}\sqrt{\frac{\rho_s}{\rho}\frac{G_s}{G}}\right), \tag{2b}$$

where G is the soil shear modulus, r_0 is the base radius for circular bases or the equivalent radius $\left(\sqrt{A/\pi}\right)$ for non-circular bases, ρ is the soil density, l is the embedment depth, and G_s and ρ_s are the shear modulus and density of the side layers (backfill). The dimensionless stiffness and damping parameters C_{v1} and $\bar{C}_{v2}$ depend on the dimensionless frequency $a_0 = \omega_0 r_0/V_s$ where ω_0 is the system natural frequency and V_s is the soil shear wave velocity. S_{v1} and $\bar{S}_{v2}$ are the dimensionless stiffness and damping parameters for the side layer. Novak [1] provided values of C_{v1}, $\bar{C}_{v2}$, S_{v1} and $\bar{S}_{v2}$ that are suitable for most hammer and press applications.

2.2. Foundation on piles

The stiffness and damping of pile foundations are evaluated from the stiffness and damping of single piles modified to account for the group effect. The vertical stiffness and damping coefficients for a single pile can be calculated as [7]

$$k = \frac{E_pA_p}{R}f_{v1}, \quad c = \frac{E_pA_p}{V_s}f_{v2}, \tag{3a, b}$$

where E_p, A_p, and R are Young's modulus, cross-sectional area and radius of the pile, respectively. The dimensionless parameters f_{v1} and f_{v2} represent the soil properties and are given in charts in Ref. [7]. The stiffness and damping of a group of piles can be computed using the

approach described in Ref. [8]. In this approach, the stiffness and damping of single piles are calculated first, then the group effect is accounted for using the dynamic interaction factors introduced by Ref. [9].

2.3. Hammers on mounting systems (directly sprung)

The stiffness and damping constants of mounting systems that have springs and viscous dampers (e.g., Fig. 1(c)) depend on the material from which they are made and their configuration and are usually supplied by the manufacturer.

3. Mathematical model

The hammer foundation system shown in Fig. 1(a) and a directly sprung hammer founded on rock (similar to Fig. 1(c)) may be considered to be a one-mass foundation. The mathematical model of a one-mass foundation is shown in Fig. 2. The response of the foundation varies with time, i.e., $v = v(t)$. However, the response will be referred to as v for brevity. The governing equilibrium equation of the one mass system shown in Fig. 2 is given by

$$m\ddot{v} + c\dot{v} + kv = f(t), \tag{4}$$

where m is the mass of the foundation system, k and c are its stiffness and damping constants, v, $\dot{v}$ and $\ddot{v}$ are the displacement, velocity and acceleration of the foundation block, respectively, and $f(t)$ is the forcing function.

Applying the Laplace transform [10] to both sides of the equations yields

$$m(VS^2 - v_0S - \dot{v}_0) + c(SV - v_0) + kV = F(S), \tag{5}$$

where S is a complex variable (called complex frequency) associated with Laplace transform, V and $F(S)$ are variables equivalent to v and $f(t)$ and are functions of S, v_0 and $\dot{v}_0$ are the initial displacement and initial velocity of the foundation block, respectively. Rearranging

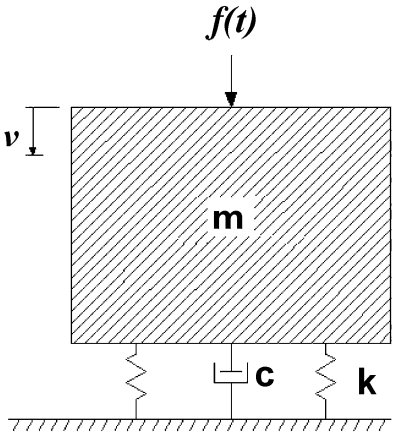

Fig. 2. One-mass foundation model.

Eq. (5) yields

$$V(S) = \frac{(mv_0 S + m\dot{v}_0 + cv_0)}{(mS^2 + cS + k)} + \frac{F(S)}{(mS^2 + cS + k)}. \tag{6}$$

The first term on the right hand side of Eq. (6) represents the transient response due to the initial conditions (termed as the zero input response) while the second term represents the response due to the applied load. The term $1/(mS^2 + cS + k)$ is the system transfer function and represents the admittance of the system (reciprocal of the impedance). The response time history is obtained by applying an inverse Laplace transform to Eq. (6).

3.1. Zero input response (homogeneous response)

The zero input response is the response of the system when no external force is applied. It exists only when there are initial conditions, displacement and/or velocity. This response is transient for most systems (i.e., damped systems) and is dependent on the system properties (mass, stiffness and damping).

For zero external load, Eq. (4) becomes

$$m\ddot{v} + c\dot{v} + kv = 0 \tag{7}$$

and consequently, Eq. (6) is reduced to

$$V(S) = \frac{(mv_0 S + m\dot{v}_0 + cv_0)}{(mS^2 + cS + k)}. \tag{8}$$

Manipulating Eq. (8) by dividing the nominator and denominator by m and completing the denominator to a complete square leads to

$$V(S) = \frac{v_0 S + \dot{v}_0 + (c/m)v_0}{(S + c/(2m))^2 + (k/m - c^2/(4m^2))}. \tag{9}$$

Introducing the natural frequency, $\omega_0 = \sqrt{k/m}$, the damping ratio, $D = c/2\sqrt{km}$ and the damped natural frequency, $\omega_0' = \omega_0\sqrt{1 - D^2}$, and then substituting into Eq. (8) and rearranging yields

$$V(S) = \frac{v_0 S + \dot{v}_0 + 2D\omega_0 v_0}{(S + D\omega_0)^2 + (\omega_0')^2}. \tag{10}$$

Applying an inverse Laplace transform to Eq. (10) gives

$$v(t) = v_0 e^{-D\omega_0 t}\cos(\omega_0' t) + \left(\frac{\dot{v}_0}{\omega_0'} + \frac{D}{\sqrt{1 - D^2}} v_0\right) e^{-D\omega_0 t}\sin(\omega_0' t). \tag{11}$$

The velocity is obtained by differentiating the displacement, i.e.,

$$\dot{v}(t) = \dot{v}_0 e^{-D\omega_0 t}\cos(\omega_0' t) - \left(\frac{\omega_0}{\sqrt{1 - D^2}} v_0 + \frac{D}{\sqrt{1 - D^2}} \dot{v}_0\right) e^{-D\omega_0 t}\sin(\omega_0' t). \tag{12}$$

3.2. Initial velocity approach

If the duration of the impact load, t_p, is very short relative to the natural period of the machine-foundation system, $T = 2\pi/\omega_0$ (i.e., $t_p \ll T$), it can be assumed that the load will expire before the system starts to respond. In this case, $f(t)$ is assumed to be zero and the foundation goes through a free vibration triggered by an initial velocity, $\dot{v}_0$. The response is obtained by using Eq. (11) and setting the initial displacement of the foundation block, v_0, to zero, i.e.,

$$v(t) = \frac{\dot{v}_0}{\omega_0'} e^{-D\omega_0 t} \sin(\omega_0' t). \tag{13}$$

The velocity becomes

$$\dot{v}(t) = \dot{v}_0 e^{-D\omega_0 t} \cos(\omega_0' t) - \frac{\dot{v}_0 D}{\sqrt{1-D^2}} e^{-D\omega_0 t} \sin(\omega_0' t). \tag{14}$$

The initial velocity, $\dot{v}_0$, can be obtained from consideration of the collision between the hammer head and the foundation. The pulse resulting from this collision is presumed to be infinitesimally short and, as a result, the restoring and damping forces have not been activated during the collision. Consequently, the collision is governed by the relations valid for two free bodies and the initial velocity can be evaluated from considerations of conservation of momentum. The maximum response occurs at a time t_m given by

$$t_m = \frac{1}{\omega_0'} \arctan \frac{\sqrt{1-D^2}}{D}. \tag{15}$$

The maximum response of the foundation system is obtained by substituting t_m in Eq. (13). The force transmitted to the foundation base (soil or piles) can be evaluated from

$$f_s(t) = kv + c\dot{v}. \tag{16}$$

3.3. Response to applied loads

If the duration of the impact load is greater than one-tenth the natural period of the machine-foundation system (i.e., $t_p \ll T$), the response of the system is affected by the characteristics of the impact load. The impact load is characterized by its amplitude, form of variation with time and duration, or its impact energy. The impact energy is evaluated as the integration of the time history of the forcing function. The following sections examine the system response to various impact loads.

3.3.1. Rectangular pulse

The rectangular pulse load is characterized by constant amplitude, P_r, during the load period, t_p, and is equal to zero outside this period as shown in Fig. 3(a). The time history of a rectangular pulse load is expressed as

$$f(t) = \begin{cases} P_r, & 0 < t < t_p, \\ 0, & t > t_p. \end{cases} \tag{17}$$

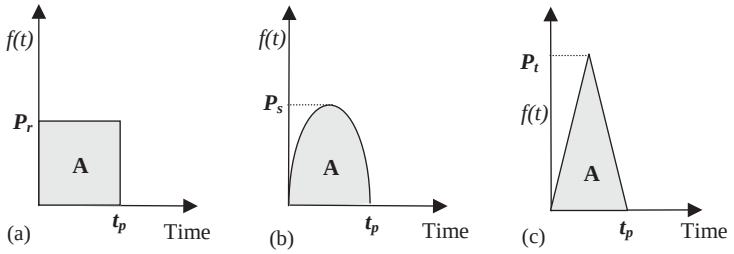

Fig. 3. Different shapes of pulse loads: (a) rectangular, (b) half-sine, (c) triangular.

The Laplace transform of the pulse is

$$F(S) = \begin{cases} \dfrac{P_r}{S}, & 0 < t < t_p, \\ 0, & t > t_p. \end{cases} \tag{18}$$

Substituting Eq. (18) into Eq. (6) and setting the initial conditions to zero, it can be shown that

$$V(S) = \frac{P_r}{k}\left[\frac{1}{S} - \frac{S + c/m}{(S + D\omega_0)^2 + (\omega_0')^2}\right]. \tag{19}$$

Applying an inverse Laplace transform to Eq. (19) yields

$$v(t) = \frac{P_r}{k}\left[1 - \mathrm{e}^{-D\omega_0 t}\cos(\omega_0' t) - \frac{D}{\sqrt{1-D^2}}\mathrm{e}^{-D\omega_0 t}\sin(\omega_0' t)\right], \quad 0 < t < t_p, \tag{20}$$

and the velocity is given by

$$\dot{v}(t) = \frac{P_r}{k}\left[\frac{\omega_0}{\sqrt{1-D^2}}\mathrm{e}^{-D\omega_0 t}\sin(\omega_0' t)\right], \quad 0 < t < t_p. \tag{21}$$

When the pulse expires, the system goes through free vibration, which is only influenced by its damped natural frequency and displacement and velocity at the end of the pulse. The solution for this free vibration is similar to the solution of the zero input response case (Section 3.1) with the initial conditions (displacement and velocity) being calculated from Eqs. (20) and (21) by setting t to t_p. Hence, the time history of the response after the load duration is expressed as

$$\begin{aligned} v(t) = {} & v_{t_p}\mathrm{e}^{-D\omega_0(t-t_p)}\cos(\omega_0'(t-t_p)) \\ & + \left(\frac{D\omega_0 v_{t_p} + \dot{v}_{t_p}}{\omega_0'}\right)\mathrm{e}^{-D\omega_0(t-t_p)}\sin(\omega_0'(t-t_p)), \quad t > t_p, \end{aligned} \tag{22}$$

$$\begin{aligned} \dot{v}(t) = {} & \dot{v}_{t_p}\mathrm{e}^{-D\omega_0(t-t_p)}\cos(\omega_0'(t-t_p)) \\ & - \left(\frac{\omega_0}{\sqrt{1-D^2}}v_{t_p} + \frac{D}{\sqrt{1-D^2}}\dot{v}_{t_p}\right)\mathrm{e}^{-D\omega_0(t-t_p)}\sin(\omega_0'(t-t_p)), \quad t > t_p, \end{aligned} \tag{23}$$

where v_{t_p} and $\dot{v}_{t_p}$ are the displacement and velocity of the foundation block at the end of the pulse ($t = t_p$). Usually, the duration of the impact load is much shorter than the system natural period

and the maximum response occurs after the end of the pulse. The force transmitted to the supporting medium can be evaluated using Eq. (16).

3.3.2. Half-sine pulse

The half-sine pulse can be described by its amplitude P_s and its duration t_p as shown in Fig. 3(b). The pulse time history is expressed as

$$f(t) = \begin{cases} P_s \sin\left(\frac{\pi}{t_p} t\right) = P_s \sin(\omega t), & 0 < t < t_p, \\ 0, & t > t_p, \end{cases} \tag{24}$$

where $\omega = \pi/t_p$. The Laplace transform of the pulse is

$$F(S) = \begin{cases} \frac{P_s \pi/t_p}{S^2 + (\pi/t_p)^2} = \frac{P_s \omega}{S^2 + \omega^2}, & 0 < t < t_p, \\ 0, & t > t_p. \end{cases} \tag{25}$$

Substituting Eq. (25) in Eq. (6) and setting the initial conditions to zero gives the response during the pulse period in the complex frequency domain, i.e.,

$$V(S) = \frac{P_s \omega}{S^2 + \omega^2} \frac{1}{mS^2 + cS + k} = \frac{P_s \omega/m}{(S^2 + \omega^2)(S^2 + 2D\omega_0 S + \omega_0')}. \tag{26}$$

The foundation response during the pulse period is obtained by applying an inverse Laplace transform to Eq. (26), i.e.,

$$\begin{aligned} v(t) = \frac{P_s \omega/m}{(\omega^2 - \omega_0^2)^2 + 4D^2\omega_0^2\omega^2} \Bigg[& -2D\omega_0 \cos(\omega t) + \frac{\omega_0^2 - \omega^2}{\omega} \sin(\omega t) \\ & + 2D\omega_0 e^{-D\omega_0 t} \cos(\omega_0' t) + \left(\frac{\omega^2 - \omega_0^2 + 4D^2\omega_0^2}{\omega_0'}\right) e^{-D\omega_0 t} \sin(\omega_0' t) \Bigg]. \end{aligned} \tag{27}$$

The velocity is obtained by differentiating the displacement, i.e.,

$$\begin{aligned} \dot{v}(t) = \frac{P_s \omega/m}{(\omega^2 - \omega_0^2)^2 + 4D^2\omega_0^2\omega^2} \Bigg[& 2D\omega\omega_0 \sin(\omega t) + (\omega^2 - \omega_0^2) e^{-D\omega_0 t} \cos(\omega_0' t) \\ & + (\omega_0^2 - \omega^2) \cos(\omega t) - \left(2D\omega_0\omega_0' + \frac{(\omega^2 - \omega_0^2 + 2D^2\omega_0^2)D}{\sqrt{1 - D^2}}\right) e^{-D\omega_0 t} \sin(\omega_0' t) \Bigg]. \end{aligned} \tag{28}$$

The displacement and velocity of the system at the end of the pulse, $v(t_p)$ and $\dot{v}(t_p)$, are calculated by replacing t with t_p in Eqs. (27) and (28), and are used as initial conditions in Eqs. (22) and (23) to find the response of the system after the end of the pulse.

3.3.3. Triangular pulse

The symmetric triangular pulse is shown in Fig. 3(c) and its time history is expressed as

$$f(t) = \begin{cases} \dfrac{2P_t}{t_p}t, & 0 < t < \frac{1}{2}t_p, \\ 2P_t\left(1 - \dfrac{t}{t_p}\right), & \frac{1}{2}t_p < t < t_p, \\ 0, & t > t_p. \end{cases} \tag{29}$$

The response can be found over three stages as follows.

First stage ($0 < t < \frac{1}{2}t_p$): The Laplace transform of the forcing function during the first stage is given by

$$F(S) = \frac{2P_t}{t_p}\frac{1}{S^2}. \tag{30}$$

Substituting Eq. (30) into Eq. (6) and setting the initial conditions to zero gives

$$V(S) = \frac{2P_t}{t_p}\frac{1}{S^2}\frac{1}{mS^2 + cS + k} = \frac{2P_t}{mt_p}\frac{1}{S^2(S^2 + 2D\omega_0 S + \omega_0^2)}. \tag{31}$$

Applying an inverse Laplace transform to Eq. (31) yields

$$v(t) = \frac{P_t}{kt_p}\left[\frac{-4D}{\omega_0} + 2t + \frac{4D}{\omega_0}e^{-D\omega_0 t}\cos(\omega_0' t) + \frac{4D^2 - 2}{\omega_0'}e^{-D\omega_0 t}\sin(\omega_0' t)\right]. \tag{32}$$

The velocity during this stage is obtained by differentiating Eq. (32), i.e.,

$$\dot{v}(t) = \frac{2P_t}{kt_p}\left[1 - e^{-D\omega_0 t}\cos(\omega_0' t) - \frac{D}{\sqrt{1 - D^2}}e^{-D\omega_0 t}\sin(\omega_0' t)\right], \quad 0 < t < \tfrac{1}{2}t_p. \tag{33}$$

The displacement and velocity at the end of first stage, $v_{(1/2)t_p}$ and $\dot{v}_{(1/2)t_p}$, are calculated by substituting $\frac{1}{2}t_p$ in Eqs. (32) and (33) and are used as initial conditions for the second stage of the pulse.

Second stage ($\frac{1}{2}t_p < t < t_p$): The total response during the second stage is obtained by summing the response due to the impact load during this stage (load-induced response) and the response due to the initial conditions at the beginning of the stage (free vibration response), i.e.,

$$v(t) = v_1(t) + v_2(t), \quad \tfrac{1}{2}t_p < t < t_p, \tag{34}$$

where $v_1(t)$ is the load-induced response and $v_2(t)$ is the free vibration response.

The impact load during the second stage can be considered as the sum of a constant load with amplitude $2P_t$ and a negative ramp load given by $-2P_t/t_p t$. The load-induced response can then be obtained by superimposing the responses due to both loads.

The load-induced response is obtained by subjecting the two load components to the Laplace transform, substituting in Eq. (6) and setting the initial conditions to zero. The response time history, $v_1(t)$, is then obtained by applying an inverse Laplace transform to the resulting equation

and is given by

$$v_1(t) = \frac{P_t}{k}\left[1 + \frac{4D}{\omega_0 t_p} - \frac{2}{t_p}\left(t - \tfrac{1}{2}t_p\right) - \left(1 + \frac{4D}{\omega_0 t_p}\right)e^{-D\omega_0(t-(1/2)t_p)}\cos\left(\omega_0'\left(t - \tfrac{1}{2}t_p\right)\right) - \left(\frac{D}{\sqrt{1-D^2}} + \frac{4D^2-2}{\omega_0' t_p}\right)e^{-D\omega_0(t-(1/2)t_p)}\sin\left(\omega_0'\left(t - \tfrac{1}{2}t_p\right)\right)\right]. \quad (35)$$

The free vibration response during the second stage is calculated using the initial conditions $v_{(1/2)t_p}$ and $\dot{v}_{(1/2)t_p}$ obtained at the end of the first stage. The free vibration response during the second stage, $v_2(t)$, is given by

$$v_2(t) = v_{(1/2)t_p}e^{-D\omega_0(t-(1/2)t_p)}\cos\left(\omega_0'\left(t - \tfrac{1}{2}t_p\right)\right) + \left(\frac{D\omega_0 v_{(1/2)t_p} + \dot{v}_{(1/2)t_p}}{\omega_0'}\right)e^{-D\omega_0(t-(1/2)t_p)}\sin\left(\omega_0'\left(t - \tfrac{1}{2}t_p\right)\right). \quad (36)$$

The velocity during the second stage is obtained by differentiating the displacement with respect to time, i.e.,

$$\dot{v}(t) = \dot{v}_1(t) + \dot{v}_2(t), \quad \tfrac{1}{2}t_p < t < t_p, \quad (37)$$

where

$$\dot{v}_1(t) = \frac{P_t}{k}\left[-\frac{2}{t_p} + \frac{2}{t_p}e^{-D\omega_0(t-(1/2)t_p)}\cos\left(\omega_0'\left(t - \tfrac{1}{2}t_p\right)\right) + \left(\frac{2D/t_p + \omega_0}{\sqrt{1-D^2}}\right)e^{-D\omega_0(t-(1/2)t_p)}\sin\left(\omega_0'\left(t - \tfrac{1}{2}t_p\right)\right)\right], \quad (38)$$

$$\dot{v}_2(t) = \dot{v}_{(1/2)t_p}e^{-D\omega_0(t-(1/2)t_p)}\cos\left(\omega_0'\left(t - \tfrac{1}{2}t_p\right)\right) - \left(\frac{\omega_0}{\sqrt{1-D^2}}v_{(1/2)t_p} + \frac{D}{\sqrt{1-D^2}}\dot{v}_{(1/2)t_p}\right)e^{-D\omega_0(t-(1/2)t_p)}\sin\left(\omega_0'\left(t - \tfrac{1}{2}t_p\right)\right). \quad (39)$$

The response at the end of the second stage v_{t_p} and $\dot{v}_{t_p}$ is used as the initial conditions for the third stage.

Third stage ($t > t_p$): The system vibrates freely after the end of the pulse ($f(t) = 0$). Eqs. (22) and (23) can be used to calculate the response of the foundation system using v_{t_p} and $\dot{v}_{t_p}$ evaluated at the end of the second stage.

4. Numerical example

A shallow foundation is designed to support a forging hammer. The foundation is square in plan 5 m × 5 m and is 2 m thick. The foundation is fully embedded in the soil (i.e., $l = 2$ m). The soil profile at the foundation site consists of fairly homogeneous cohesive soil with an average shear wave velocity 150 m/s and mass density 1900 kg/m^3. The total mass of the foundation and supported equipment is 200,000 kg. The backfill material (the side soil layer) is granular A with an average shear wave velocity of 120 m/s and a mass density of 1800 kg/m^3. The stiffness and

damping constants of the foundation calculated using Eq. (2) are $k = 8.1 \times 10^8$ N/m, $c = 1.0 \times 10^7$ N/m/s.

The dynamic characteristics of the foundation system are calculated for the given values of k, c and m as

$$\omega_0 = 63.6 \text{ rad/s}, \quad D = 39.3\%, \quad \omega_0' = 58.5 \text{ rad/s}.$$

The impact force due to the forging act of the hammer is modelled as a rectangular, half-sine or triangular pulse with a period of 10 ms and constant power content (area under the load-time curve). The amplitude of the rectangular pulse considered in this example is $P_r = 1$ MN. The amplitude of a half-sine pulse that has the same power (area under load-time curve) and duration as the rectangular pulse is obtained by equating the power of the two pulses, i.e.,

$$\int_0^{t_p} P_s \sin\left(\frac{\pi}{t_p} t\right) dt = P_r t_p. \tag{40}$$

Solving for the amplitude of the half-sine pulse, P_s, gives

$$P_s = \frac{P_r \pi}{2}. \tag{41}$$

Similarly, the amplitude of a triangular pulse, P_t, is obtained using the same method to maintain the same duration and power of the impact and is given by

$$P_t = 2P_r. \tag{42}$$

The response of the foundation system to the rectangular pulse load is evaluated first using the equations developed and the displacement response is compared in Fig. 4 with the numerical solution of the response obtained by solving the governing equilibrium equation (Eq. (4)) using the Runge–Kutta formula, Dormand–Prince pair with variable step size [12]. Fig. 4 shows that the responses obtained from both methods are almost identical, confirming the validity of the developed equations.

The response of the foundation system to the three forms of the impact load is evaluated using the equations developed and the results are presented in Figs. 5–7. Fig. 5 shows the displacement of the foundation system to the three load types. It is noted from the figure that for the case considered (short load duration) the system response is almost the same for all load types considered. Similar observations can be made from Figs. 6 and 7 for the velocity of the foundation and the force transmitted to the soil, respectively.

5. Effect of pulse duration

Since the exciting forces due to a mill or a hammer operation are stochastic in nature, design codes (e.g., Ref. [11]) require that the maximum size of representative excitation processes (e.g., individual impacts) be estimated where no excitation time history or power spectrum functions exist. This maximum size impact is always specified as the design load for the foundation system, and usually the duration is not provided. The maximum size impact is usually associated with extreme events that maximize the load amplitude but the duration of the impact is usually short. However, the same machine at different operating conditions may produce different size impacts

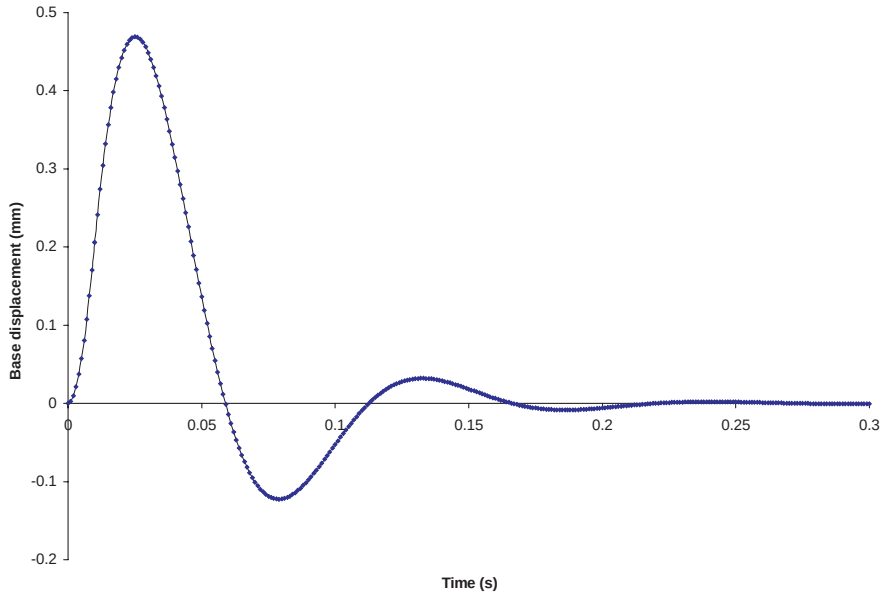

Fig. 4. Response of a one-mass hammer foundation system to a 10 ms rectangular pulse: —, analytical; ♦, numerical solutions.

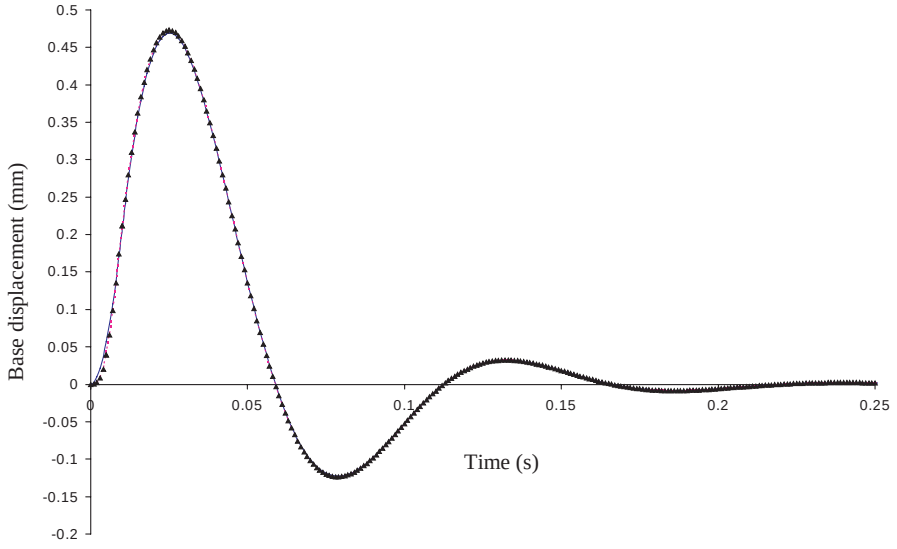

Fig. 5. Displacement time history due to 10 ms pulse: —, rectangular; - - -, half-sine; ▲, triangular.

that can be characterized by smaller amplitudes but longer durations when compared with maximum size impacts.

For example, the maximum size impact in forging hammers occurs when the sample is absent thus yielding the hardest shock but for a short duration. However, the lowest impact size occurs

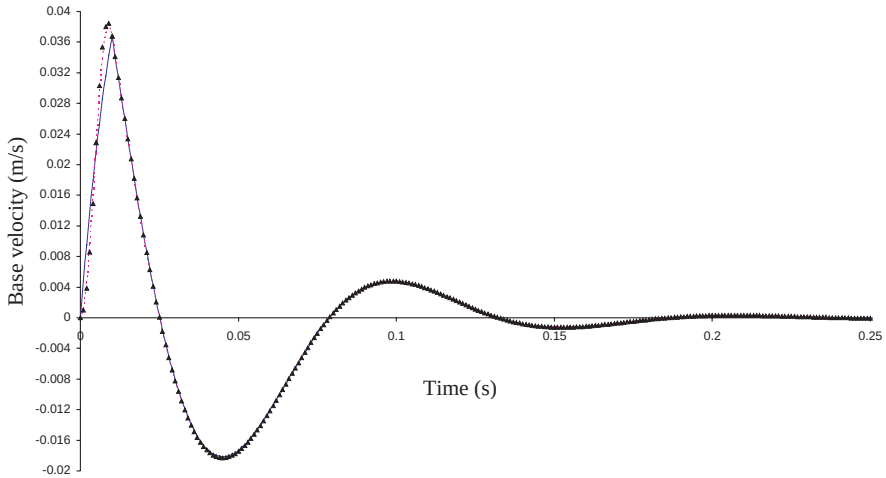

Fig. 6. Velocity time history due to 10 ms pulse: —, rectangular; - - -, half-sine; ▲, triangular.

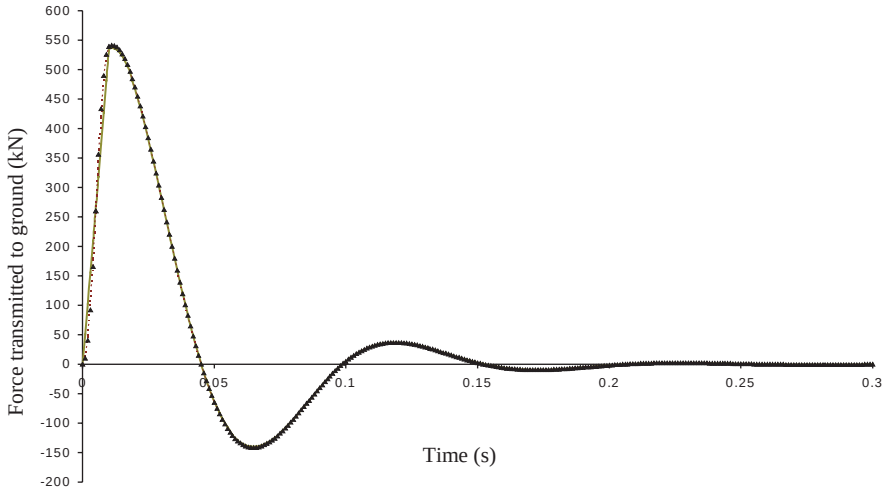

Fig. 7. Time history of force transmitted to ground due to 10 ms pulse: —, rectangular; - - -, half-sine; ▲, triangular.

when forging nonferrous materials but the duration will be much longer. Similarly, in clinker mills the size of impact (due to the grinding process) and its duration depend on the size of the feed aggregate. Large aggregates with a small percentage of fines will lead to the largest size impact but for a short duration. On the other hand, if the aggregate size is small and the percentage of fines is high, the amplitude of the impact decreases and the duration increases.

In both cases, the power of the impact should only depend on the capacity of the exciter of the machine, which is presumed to be constant or limited to a maximum value depending on its mechanical design. Therefore, it is of interest to examine the effect of the impact duration on the system response. Thus, the three forms of the impact load considered in this study (i.e., rectangular, half-sine and triangular) with the same power content but with a duration of 50 ms

(rather than 10 ms) were applied to the foundation system. The results are compared with those obtained for the short duration case (i.e., 10 ms) in Figs. 8, 9 and 10 for the displacement and velocity of the foundation, and the force transmitted to the soil, respectively. The figures show that the responses decreased for the long period case for all load forms but by varying amounts. For the long period case, the responses due to the rectangular pulse are smaller than those for the half-sine pulse, which in turn are smaller than those for the triangular pulse.

To further examine the effect of pulse duration (and its form) on system behaviour, the pulse duration was varied from very short (almost zero) duration to a duration that is five times the system natural period while keeping the impact power content constant. The response was calculated in each case and the maximum responses (displacement and velocity of the foundation, and the force transmitted to the soil) were recorded. The maximum response was then normalized by the maximum response due to a very short pulse ($t_p \approx 0$) and the pulse duration was normalized by the foundation natural period ($T = 1/f$). The results are presented in Figs. 11, 12 and 13 for the displacement and velocity of the foundation, and the force transmitted to the soil or piles.

Fig. 11 shows that the response of the system decreases as the pulse duration increases (for constant power content). For example, the foundation response for a pulse with $t_p = \frac{1}{2}T$ is 55–75% of the foundation response due to a pulse $t_p \ll T$, and its response due to a pulse with $t_p = T$ is 30–50% the response due to the short duration pulse. It can also be noted from Fig. 11 that the assumed form of the impact load has a significant effect on the calculated response for a long duration pulse. For example, for a pulse with $t_p = T$ the response of the foundation to a triangular pulse is 50% higher than its response to a rectangular pulse. Similar observations can be made regarding the foundation velocity and the force transmitted to the soil from Figs. 12 and 13.

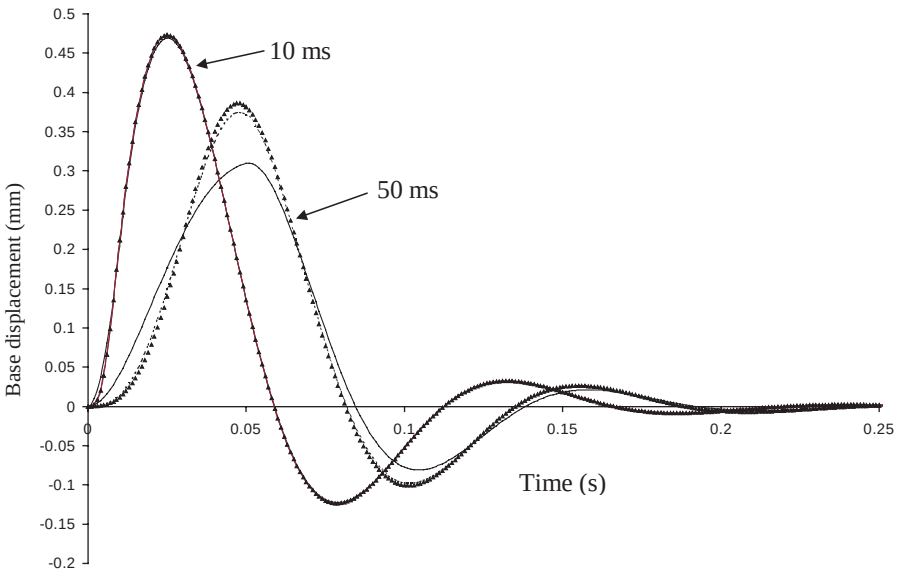

Fig. 8. Displacement time history due to 10 and 50 ms pulses: —, rectangular; - - -, half-sine; ▲, triangular.

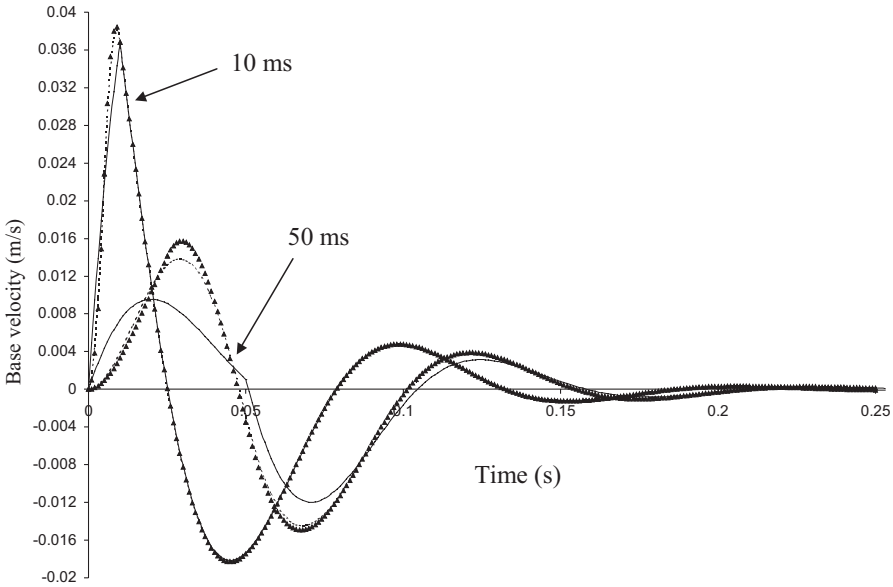

Fig. 9. Velocity time history due to 10 and 50 ms pulses: —, rectangular; - - -, half-sine; ▲, triangular.

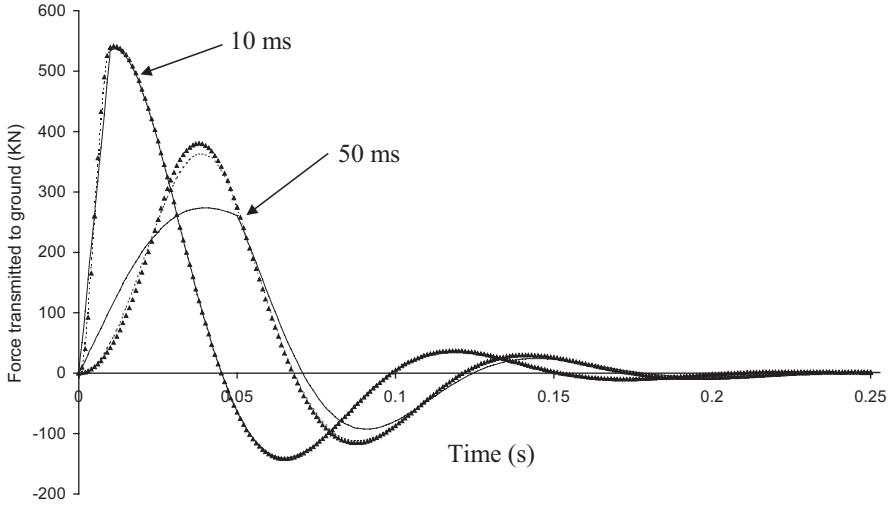

Fig. 10. Time history of forces transmitted to ground due to 10 and 50 ms pulses: —, rectangular; - - -, half-sine; ▲, triangular.

The system response is sensitive to the pulse duration for $t_p < 2T$. For $t_p > 2T$, the response becomes insensitive to the pulse durations. For long pulses, the problem converges to the static case (note that the velocity amplitude converges to zero as the pulse duration increases).

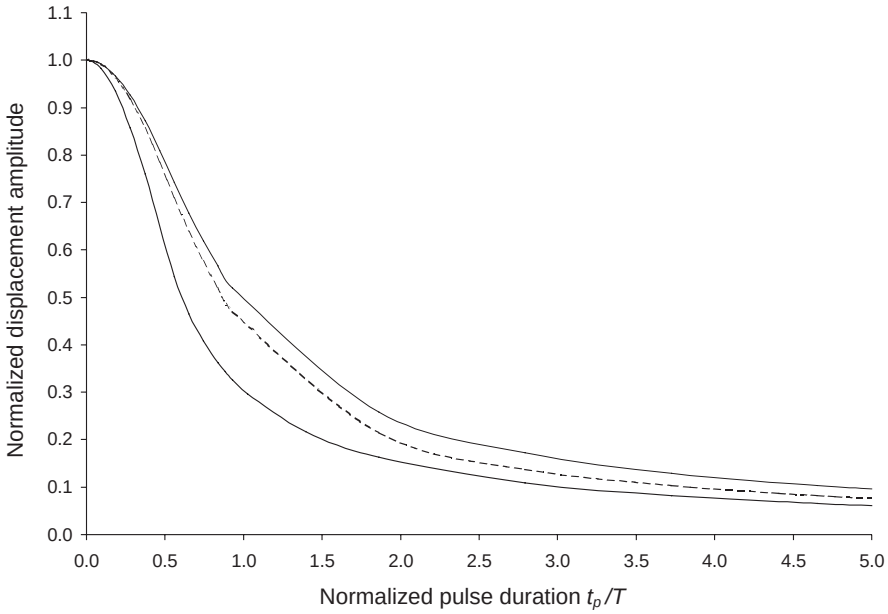

Fig. 11. Effect of pulse duration on the vibration amplitude: —, rectangular; - - - - -, half-sine; ....., triangular.

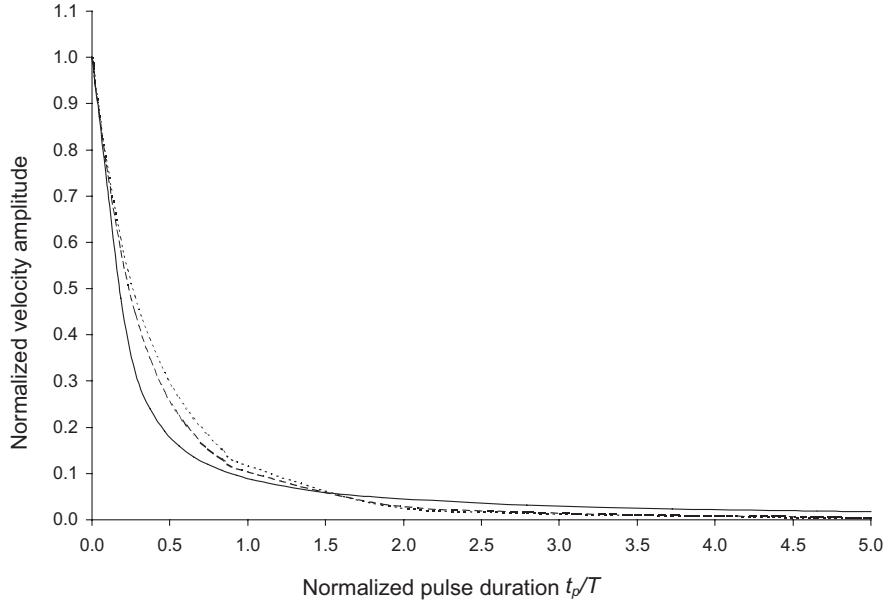

Fig. 12. Effect of pulse duration on the maximum velocity: —, rectangular; - - - - -, half-sine; ....., triangular.

6. Conclusions

Closed form solutions for the evaluation of a one-mass foundation response to rectangular, half-sine and triangular pulses have been developed and expressed in terms of the system dynamic

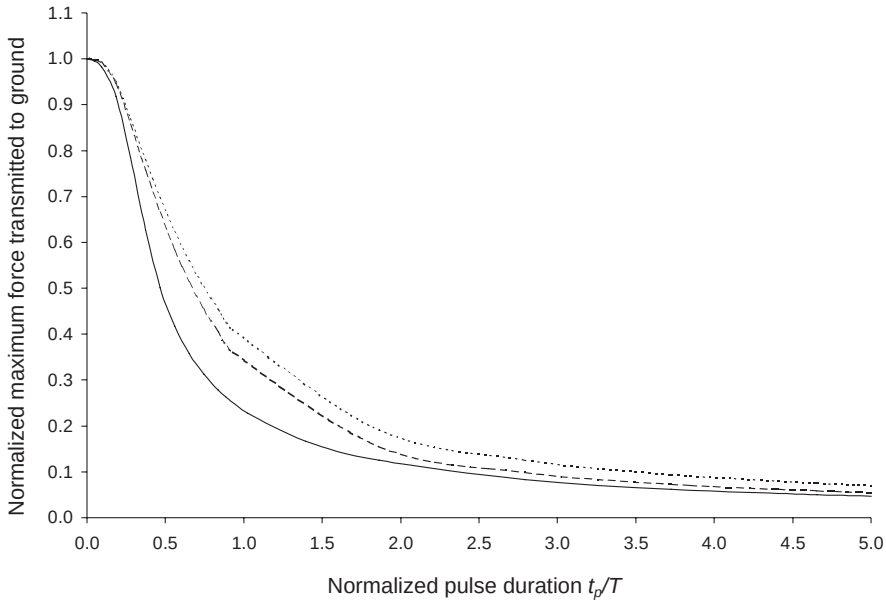

Fig. 13. Effect of pulse duration on the maximum base force: —, rectangular; - - - - -, half-sine; ....., triangular.

characteristics and the pulse properties. The results from the developed solutions compared well with the numerical solution. The developed equations were used to evaluate the response of a one-mass foundation to pulse loading with different shapes and/or pulse duration but constant power content. The following conclusions were made:

1. For short pulse duration ($t_p < T/10$), the foundation response is insensitive to the pulse form. The response is almost the same for all pulse forms.
2. As the pulse duration increases, the system response decreases. Therefore, prolonging the pulse duration (relative to the period of the system) helps reduce the dynamic response of hammer and mill foundations (for constant power content). Thus, a properly designed mounting system may be used to alter the system period and the rate of load, and consequently reduces the system response.
3. For long pulse duration, the triangular pulse results in a higher response compared to half-sine and rectangular pulses. Therefore, it is safer to consider a triangular pulse in the response analyses of hammer and mill foundations.
4. For very long pulse duration ($t_p > 2T$), the response becomes insensitive to the pulse duration.

References

[1] M. Novak, Foundations of shock-producing machines, *Canadian Geotechnical Journal* 20 (1) (1983) 141–158.
[2] M. Novak, L. El Hifnawy, Vibration of hammer foundations, *Soil Dynamics and Earthquake Engineering* 2 (1) (1983) 43–53.

[3] L. El Hifnawy, M. Novak, Response of hammer foundations to pulse loading, *Soil Dynamics and Earthquake Engineering* 3 (3) (1984) 124–132.
[4] A. Chehab, M.H. El Naggar, Design of efficient base isolation for hammers and presses, *Soil Dynamics and Earthquake Engineering* 23 (2) (2003) 127–141.
[5] Y.O. Beredugo, M. Novak, Coupled horizontal and rocking vibration of embedded footings, *Canadian Geotechnical Journal* 9 (4) (1972) 477–497.
[6] M. Novak, Effect of soil on structural response to wind and earthquake, *Earthquake Engineering and Structural Dynamics* 3 (1) (1974) 79–96.
[7] M. Novak, Dynamic stiffness and damping of piles, *Canadian Geotechnical Journal* 11 (4) (1974) 574–598.
[8] M.H. El Naggar, M. Novak, Nonlinear lateral interaction in pile dynamics, *Soil Dynamics and Earthquake Engineering* 14 (2) (1995) 141–157.
[9] A.M. Kaynia, E. Kausel, Dynamic behaviour of pile groups, *Conference on Numerical Methods in Offshore Pilling*, The University of Texas, Austin, TX, 1982, pp. 509–532.
[10] C.M. Close, D.K. Frederick, *Modeling and Analysis of Dynamic Systems*, 2nd Edition, Houghton Mifflin, Boston, MA, 1993, pp. 250–299 (Chapter 7).
[11] DIN 4024, German Code for the Design of Machine Foundations.
[12] P.V. O'Neil, *Advanced Engineering Mathematics*, 4th Edition, Thomson, Stamford, CT, 1994, pp. 189–216 (Chapter 5).